Zhang et al. BMC Medical Informatics and Decision Making (2025) 25:159
https://doi.org/10.1186/s12911-025-02987-9

BMC Medical Informatics and Decision Making

RESEARCH

Open Access

Development of machine learning models to predict the risk of fungal infection following flexible ureteroscopy lithotripsy

Haofang Zhang[1,2], Changbao Xu[1,2*], Chenge Hu[2], Yunlai Xue[2], Daoke Yao[2], Yifan Hu[1,2], Ankang Wu[2], Miao Dai[2] and Hang Ye[2]

Abstract

Background The flexible ureteroscopy lithotripsy (F-URL) is an important treatment for upper urinary tract stones. However, urolithiasis, surgical procedures, and catheter placement are risk factors for fungal infections. Our study aimed to construct a machine learning algorithm predictive model to predict the risk of fungal infection following F-URL.

Methods This study retrospectively collected the clinical data of patients who underwent F-URL at the Second Affiliated Hospital of Zhengzhou University from January 2016 to March 2024. The patients were divided into a non-fungal infection group and a fungal infection group based on whether a fungal infection occurred within three months post-surgery. The patient data from January 2016 to December 2023 were used as training data, and the patient data from January 2024 to March 2024 were used as testing set. The training data was randomly divided into a training set and validation set at a ratio of 90:10. Use LASSO regression to screen clinical features based on the training set. Nine machine learning algorithms, Logistic Regression (LR), k-Nearest Neighbours (KNN), Support Vector Machines (SVM), Random Forest (RF), Categorical Boosting (CatBoost), eXtreme Gradient Boosting (XGBoost), Adaptive Boosting (AdaBoost), Gradient Boosting Machines (GBM), and Neural Network (NNet), were used to construct models. The performance of these nine models was evaluated and the best predictive model was selected based on the validation set, and evaluate the best predictive model's generalization ability using the testing set. Visualize the constructed optimal machine learning model using the SHapley additive interpretation (SHAP) value method. SHAP force plots were established to show the application of the prediction model at the individual level.

Results A total of 13 clinical features were used to construct predictive models: age, diabetes mellitus (DM), history of malignancy, being bedridden, admission white blood cells (WBC), preoperative ureteral stenting, operation time, postoperative fever, postoperative Neu, carbapenem antibiotics use, duration of antibiotic therapy, length of hospital stay (LOS), and postoperative stent duration. Comparing the performance of 9 prediction models, we found that the model constructed using XGBoost algorithm had the best performance. The model constructed using XGBoost algorithm shows good discrimination, generalization and clinical applicability in the testing set.

*Correspondence:
Changbao Xu
xcb1966@126.com

Full list of author information is available at the end of the article

Conclusions The XGBoost model developed in this study has good predictive ability and clinical applicability for evaluating the risk of fungal infection following F-URL.

Keywords Flexible ureteroscopy lithotripsy, Machine learning algorithms, Fungal infection, Risk factors, XGBoost model

Introduction

Urolithiasis is a common disease in urology, and an epidemiological survey shows that the age-standardized prevalence of urolithiasis in China is 6.06%, with upper urinary tract stones accounting for 99.50% [1]. The flexible ureteroscopy lithotripsy (F-URL) is an important treatment for upper urinary tract stones. Studies have shown that urolithiasis, surgical procedures, and catheter placement are risk factors for fungal infections [2]. In recent years, with the widespread use of broad-spectrum antibiotics, the increased incidence of diabetes and malignancies, and the rise in invasive procedures, the incidence of fungal infections has steadily increased [3, 4], threatening global public health and imposing a significant economic burden.

Machine learning algorithms, part of the field of artificial intelligence, are designed to tackle big data and high-dimensional data, and have shown good performance in the medical field [5]. In recent years, machine learning algorithms have been increasingly adopted and applied in the diagnosis and treatment of urolithiasis [6–8].

Several studies have analyzed the risk factors for urological fungal infections [9–14], but the field of risk factors and predictive models for fungal infections after upper urinary tract stone surgery remains unexplored. This study aims to screen the risk factors for fungal infection following F-URL and construct predictive models using machine learning algorithms. Our research has the potential to help clinicians identify high-risk patients for fungal infections following F-URL. By guiding clinical doctors to implement personalized early prevention, early detection, and early intervention methods, the burden on patients and medical costs can be reduced.

Materials and methods

Study population

We retrospectively collected the clinical data of patients who underwent F-URL in the Department of Urology at the Second Affiliated Hospital of Zhengzhou University from January 2016 to March 2024. Inclusion criteria: age of patients not less than 18 years, diagnosed with upper urinary tract stones by CT, underwent F-URL treatment. Exclusion criterion:patients with preoperative fungal infection, patients with asymptomatic fungal urine preoperatively. The study was approved by the Ethics Committee of the Second Affiliated Hospital of Zhengzhou University (Approval No.: KY2024194). Our research process complies with the requirements of the Helsinki Declaration of the World Medical Association.

Therapeutic regimen

For patients with positive preoperative infection markers, cephalosporins or quinolone antibiotics were administered, and sensitive antibiotics were substituted in a timely manner based on drug susceptibility results. For patients with infections and severe obstructions, percutaneous nephrostomy or ureteral stent placement was used for timely kidney drainage. For patients with negative infection markers, prophylactic antibiotics were administered 30 min before surgery. Conduct a comprehensive assessment of the patient's condition to rule out surgical contraindications, such as severe cardiopulmonary insufficiency, uncorrected coagulation dysfunction, uncontrolled active urinary tract infection, urethral stricture or severe ureteral stricture, severe hip joint deformity, etc. After completing the preoperative preparations, traditional ureteral access sheath (T-UAS) or negative-pressure ureteral access sheath (NP-UAS) were selected for surgery based on the patients' anatomy, stone burden, and personal preference.

The main equipment used in the surgery includes the ureteral rigid ureteroscope (F8/9.8) produced by Wolf Company from Germany, the nickel-titanium super-slip guidewire (0.35 mm) produced by Bard Company from the United States, the ureteral access sheath (F12/14) produced by Cook Company from the United States, the electronic flexible ureteroscope (URF-V F8.8-9) produced by Olympus Company from Japan, the front-end bendable ureteral access sheath (F12/14) and the RP-U-C12 disposable electronic flexible ureteroscope produced by Pusen Medical Company from China, the stone retrieval basket produced by Boston Scientific Company from the United States, the MOSES 120 W holmium laser lithotripsy machine produced by Lumenis Company from the United States, and the ureteral stent (F5/7) produced by Cook Company from the United States.

After undergoing endotracheal intubation under general anesthesia, the patient was placed in the lithotomy position and an F8/9.8 Wolf ureteroscope was introduced into the bladder under direct vision. Guided by a hydrophilic guide wire, the ureteroscope was advanced to the upper ureter to observe its condition. After leaving the guide wire in place, the ureteroscope was withdrawn. Subsequently, a flexible ureteroscope sheath was inserted along the hydrophilic guide wire, followed by the placement of the flexible ureteroscope. For patients utilizing a negative pressure suction sheath, a perfusion pump was employed, with the suction pressure set at 100 ~ 200 mmHg (1 mmHg = 0.133kPa). Water was continuously infused using a pressure pump, with a flow rate of 150 ~ 200 mL/min. For patients with a common ureteral sheath, manual water injection was performed using a syringe. Laser lithotripsy was the primary method employed during the procedure. During the procedure, the holmium laser parameters were adjusted according to the size, location, and hardness of the stones, with an energy range of 0.2–2.0 J, a frequency of 5–20 Hz, and a power of 5–24 W. In cases of lower calyceal calculi with excessive stone burden or a steep infundibulum angle, the stone basket was used as necessary.

All surgeries were performed by senior urologists with extensive experience, and ureteral stents or catheters were placed as needed. Postoperatively, patients without infection were given prophylactic antibiotics only. Patients with postoperative infections were treated with cephalosporins or quinolone antibiotics, and in cases of severe infections such as urosepsis, carbapenem antibiotics were administered, with sensitive antibiotics substituted as per drug susceptibility results.

For patients without bladder outlet obstruction and no postoperative complications, the urinary catheter was removed within 24 h after surgery. For patients with bladder outlet obstruction or postoperative fever, the indwelling time of the urinary catheter was appropriately extended, with a maximum of 7 days. This was the treatment protocol followed at our center. For patients without ureteral strictures, significant ureteral damage, or CSRF, the ureteral stent was left in place for 1–2 weeks. For patients with ureteral strictures or severe postoperative infections, the ureteral stent retention time was appropriately extended, up to a maximum of 3 months.

Data collection

The collected data includes fIve types. General data, including sex (Female), age, body mass index (BMI), diabetes mellitus (DM), history of malignancy, being bedridden, long-term immunosuppressive therapy. Preoperative data, including admission hemoglobin (HB), admission white blood cells (WBC), admission neutrophils (Neu), admission alanine transaminase (ALT), admission aspartate transaminase (AST), admission albumin (ALB), admission serum creatinine (Scr), admission glycated hemoglobin (HbA1c), admission cholesterol, Pyuria, urine pH, urinary nitrite, urine culture, number of stones (Multiple stones), maximum stone diameter, peak stone density (PSD), grading of hydronephrosis, percutaneous nephrostomy (PNS), ureteral stenting. Intraoperative data, including operation time, kind of UAS. Postoperative data, including temperature (Fever), postoperative WBC, postoperative Neu, postoperative C-reactive protein (CRP), postoperative procalcitonin (PCT), and postoperative serum calcium (Ca), residual stones, stone composition (Infectious stones), urethral catheterization duration, stent duration. Other data, including carbapenem antibiotics use, duration of antibiotic therapy, length of hospital stay (LOS).

The biochemical indicators in the preoperative data were derived from the results within 24 h of admission. The biochemical indicators in the postoperative data were derived from the results 2 h after surgery.

According to the diagnostic criteria for diabetes mellitus established by the World Health Organization (WHO), DM is diagnosed if any of the following conditions are met [15, 16]: fasting plasma glucose ≥ 7.0 mmol/L; 2-h plasma glucose ≥ 11.1 mmol/L during an oral glucose tolerance test; glycated hemoglobin (HbA1c) ≥ 6.5%; or random plasma glucose ≥ 11.1 mmol/L, accompanied by classic symptoms of diabetes, such as polyuria, polydipsia, or unexplained weight loss.

Preoperative CT imaging was utilized to assess the following parameters:number of stones, maximum stone diameter, PSD, and grading of hydronephrosis. The hydronephrosis was graded by the SFU grading system [17]: Grade 0 for no hydronephrosis; Grade I for mild separation of the renal pelvis; Grade II for mild dilation of the renal pelvis with dilation of one or more calyces; Grade III for dilation of all calyces; and Grade IV for calyceal dilation with thinning of the renal parenchyma.

Considering postoperative absorptive fever, postoperative fever was defined as a temperature over 38 °C within 48 h after surgery [18]. The composition of the stones was determined using infrared spectroscopy. If the main components were struvite, carbonate apatite, or ammonium acid urate, the stones were diagnosed as infection stones [19]. The CT scan or standing abdominal X-ray was conducted within 1 month postoperatively. Residual stones exceeding 4 mm in diameter were classified as clinically significant residual fragments (CSRF) [20].

Midstream clean-catch urine samples were collected from patients, quantitative culture and identification were performed using CHROMagar Candida chromogenic medium, yeast identification strip of Remel company and API 20C AUX identification system. A fungal count ≥ 10^5 CFU/mL was diagnosed as a positive urine fungal culture result [21].

Patients were followed up for 3 months postoperatively to observe whether they developed symptoms suggestive of urinary fungal infection, such as fever and lower back pain, whether the urine fungal culture was positive, and whether antifungal treatment was effective. Based on whether the patients met all these criteria, they were divided into the fungal infection group and the non-fungal infection group.

Statistical analysis

Data analysis was performed using SPSS 23 and R 4.3.3 software. For variables with missing values less than 10%, the random forest method is used for multiple imputation, which is realized through the "mice" package in R 4.3.3 software. Variables with missing values greater than 10% were excluded. All continuous variables are non normally distributed, so we use quartiles to describe their distribution characteristics. Mann Whitney U test was used to analyze non normally distributed data. Categorical data were expressed as [n (%)], and the χ^2 test or Fisher's exact test was used for comparison, with statistical significance defined as a p value less than 0.05.

The patient data from January 2016 to December 2023 were used as training data, and the patient data from January 2024 to March 2024 were used as testing set. The training data was randomly divided into a training set and validation set at a ratio of 90:10 using R 4.3.3 software. Clinically significant features were screened by LASSO regression [22] based on the training set.

Based on the training set, we use the ten times 10-fold cross-validation method to improve the repeatability of the model. We used 9 machine learning algorithms including Logistic Regression (LR), k-Nearest Neighbours (KNN), Support Vector Machines (SVM), Random Forest (RF), Categorical Boosting (CatBoost), eXtreme Gradient Boosting (XGBoost), Adaptive Boosting (AdaBoost), Gradient Boosting Machines (GBM), and Neural Network (NNet) to construct prediction models.

ROC curves were plotted for the nine models, and their performance was evaluated using the area under the ROC curve (AUC), accuracy (ACC), sensitivity (SEN), specificity (SPE), Kappa score, F1 score, and Matthews correlation coefficient (MCC). The closer the values of the above evaluation indicators are to 1, the better the performance of the model. A study by Chicco et al. showed that MCC demonstrated reliable performance in evaluating binary classification [23]. As a result, MCC and AUC were chosen as the primary evaluation metrics for the models. The best predictive model was selected based on the validation set.

The best predictive model was selected based on the validation set. The generalization ability of the best prediction model is evaluated based on the test set. The decision curve analysis (DCA) was used to assess clinical applicability. Finally, visualize the constructed optimal machine learning model using the SHapley additive interpretation (SHAP) value method. SHAP force plots were established to show the application of the prediction model at the individual level [24].

Result

Baseline characteristics and screening of patients

A total of 4161 patient clinical records were collected, of which 7 patients were excluded due to preoperative fungal infection or preoperative asymptomatic fungal urine. In total, 4154 patients were included in this study, of whom 178 developed postoperative urinary fungal infections. Among them, there were 65 cases of Candida albicans infection, 41 cases of Candida glabrata infection, 33 cases of Candida tropicalis infection, 29 cases of Candida parapsilosis infection, 5 cases of Candida krusei infection, 2 cases of Aspergillus infection, 2 cases of Candida lusitaniae infection, and 1 case of Cryptococcus infection. Admission cholesterol, admission HbA1c, admission urine culture, postoperative CRP, and postoperative PCT were excluded due to missing data more than 10%. After multiple imputations, the remaining 36 clinical features were included in the study (Table 1).

Significant differences were found between the fungal infection group and the non-fungal infection group in sex, age, DM, history of malignancy, being bedridden, long-term immunosuppressive therapy, preoperative WBC, preoperative Neu, ALB, pyuria, urinary nitrite, preoperative Ureteral Stenting, PNS, operation time, UAS, postoperative fever, postoperative WBC, postoperative Neu, urethral catheterization duration, carbapenem antibiotics use, duration of antibiotic therapy, LOS and postoperative stent duration ($P < 0.05$).

Divide the enrolled patients into training data ($n = 3846$) and testing set (308) based on time. Randomly divide the training data into a training set ($n = 3463$) and a validation set ($n = 383$) in a ratio of 90:10 using R 4.3.3 software. Based on the training set, the remaining 36 clinical features were included in the LASSO regression to identify potential risk factors, as shown in Fig. 1. The analysis indicated that age, DM, history of malignancy, being bedridden, admission WBC, preoperative ureteral stenting, operation time, postoperative fever, postoperative Neu, carbapenem antibiotics use, duration of antibiotic therapy, LOS, and postoperative stent duration are potential risk factors of postoperative fungal infection in patients underwent F-URL.

Model development and verification

Nine prediction models were constructed using machine learning methods based on the training set, and these models were evaluated based on the validation set. The values of AUC, ACC, SEN, SPE, Kappa, MCC, and F1 score for each model are shown in Table 2, and the ROC curves are shown in Fig. 2. We can see that in the validation set, the AUC and MCC values of the model constructed using the XGBoost method are the highest, at 0.9659(95%CI: 0.9408–0.9911) and 0.5185, respectively. The XGBoost model showed the best performance in

Table 1 Comparison of clinical data between non-fungal infection group and fungal infection group

Variable	Non-fungal infection group *N* = 3976	Fungal infection group *N* = 178	χ^2/Z	P
General data				
Age (M (P25,P75), years)	50.0 (38.0,59.0)	59.0 (49.0,67.0)	−7.154	<0.001*
Female (n (%))	1571 (39.5)	106 (59.6)	28.419	<0.001*
BMI (M (P25,P75), kg/m^2)	24.8(22.8,27.7)	25.1(22.2,27.4)	−0.06	0.996
DM (n (%))	581 (14.6)	67 (37.6)	71.879	<0.001*
History of malignancy (n (%))	240 (6.0)	64 (36.0)	224.847	<0.001*
Being bedridden (*n* (%))	95 (2.4)	34 (19.1)	158.133	<0.001*
Immunosuppression (*n* (%))	26 (0.7)	12 (6.7)	63.104	<0.001*
Preoperative data				
Admission HB (M (P25,P75), g/L)	129.0 (117.0, 143.0)	129.0 (116.8, 140.0)	−1.483	0.138
Admission WBC (M (P25,P75),*109/L)	6.6 (5.1, 8.7)	7.6 (5.7, 10.1)	−4.153	<0.001*
Admission Neu (M (P25,P75),*109/L)	4.1 (3.0, 5.6)	4.7 (3.3, 7.3)	−3.197	0.001*
Admission ALB < 30 g/L (n (%))	79 (2.0)	13 (7.3)	19.848	<0.001*
Admission ALT (M (P25,P75),U/L)	19.0(13.0, 29.8)	17.0(12.0, 28.3)	−1.397	0.162
Admission AST (M (P25,P75),U/L)	15.0(11.0,19.0)	13.0(8.0, 22.0)	−1.854	0.064
Admission Scr (M (P25,P75),μmol/L)	74.0 (63.0, 92.0)	74.0 (55.0, 107.3)	−0.576	0.565
Pyuria (n (%))	3234 (81.3)	157 (88.2)	5.354	0.021*
Urinary nitrite (n (%))	129 (3.2)	17 (9.6)	19.979	<0.001*
Urine pH (M (P25,P75))	6.5 (6.0,7.0)	6.5 (6.0, 6.5)	−0.381	0.703
Multiple stones (*n* (%))	1886 (47.4)	90 (50.6)	0.668	0.414
Maximum stone diameter (M (P25,P75), mm)	10.8 (7.5, 16.5)	10.4 (8.0, 15.3)	−0.410	0.682
PSD (M (P25,P75), HU)	1275.0 (980.0, 1463.0)	1290.5 (1007.0, 1408.0)	−1.393	0.164
SFU grading (n (%))			7.559	0.109
0	644 (16.2)	18 (10.1)		
I	805 (20.2)	35 (19.7)		
II	1003 (25.2)	50 (28.1)		
III	1188 (29.9)	53 (29.8)		
IV	336 (8.5)	22 (12.4)		
Ureteral Stenting (*n* (%))	584(14.7)	59(33.1)	44.367	<0.001*
PNS (*n* (%))	34(0.9)	6(3.4)	11.306	0.006*
Intraoperative data				
Operation time (M (P25,P75), min)	53.0(31.0, 75.0)	70.0 (50.0, 111.3)	−6.849	<0.001*
UAS (*n* (%))			6.191	0.013*
T-UAS	3801(95.6)	177(99.4)		
NP-UAS	175(4.4)	1(0.6)		
Postoperative data				
Fever (n (%))	890 (22.4)	110 (61.8)	149.797	<0.001*
Postoperative WBC (M (P25,P75),*109/L)	7.0 (5.3, 9.2)	7.4 (6.2, 10.1)	−3.338	0.001*
Postoperative Neu (M (P25,P75),*109/L)	5.1 (3.2, 7.1)	6.1 (4.5,8.2)	−5.702	<0.001*
Postoperative Ca (M (P25,P75), mmol/L)	2.3 (2.3, 2.4)	2.3 (2.3,2.4)	−0.744	0.457
CSRF (n (%))	1416(35.6)	73(41.0)	2.158	0.142
Infectious stones (*n* (%))	1149 (28.9)	54 (30.3)	0.171	0.679
Urethral catheterization duration (M (P25,P75), days)	1.0 (1.0,4.0)	2.0 (1.0,4.0)	−4.105	<0.001*
Stent duration (M (P25,P75), weeks)	4.0 (4.0,8.0)	8.0 (4.0,12.0)	−7.832	<0.001*
Other data				
Carbapenem antibiotics use (*n* (%))	252 (6.3)	94 (52.8)	481.863	<0.001*
Duration of antibiotic therapy (M (P25,P75), days)	4.0 (3.0, 6.0)	8.0 (6.0, 9.0)	−14.565	<0.001*
LOS (M (P25,P75), days)	6.0 (4.0, 8.0)	12.0 (7.0, 14.0)	−13.616	<0.001*

BMI body mass index, DM diabetes mellitus, Immunosuppression long-term immunosuppressive therapy, HB hemoglobin, WBC white blood cells, Neu neutrophils, ALT alanine transaminase, AST aspartate transaminase, Scr serum creatinine, PSD peak stone density, PNS percutaneous nephrostomy, UAS ureteral access sheath, T-UAS traditional ureteral access sheath, NP-UAS negative-pressure ureteral access sheath, Ca serum calcium, CSRF clinically significant residual fragments, LOS length of hospital stay

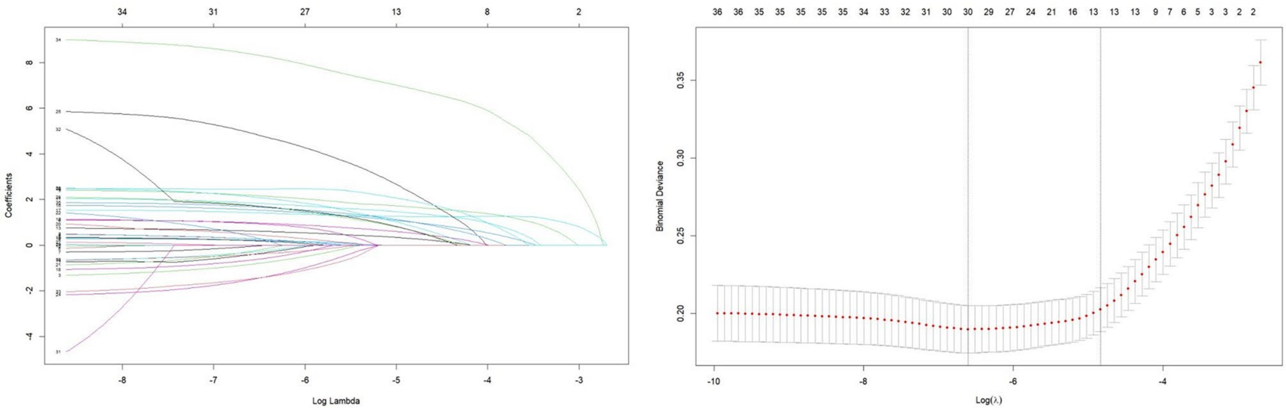

Fig. 1 Use LASSO regression to screen clinical features. **A** The LASSO coefficient path diagram shows the variation of feature coefficients corresponding to different regularization parameter (λ) values in the LASSO algorithm. **B** The cross validation results of LASSO regression show that the best model can be constructed using 13 variables

Table 2 Evaluation metrics of the models constructed by 9 machine learning algorithms

		AUC(95%CI)	ACC	SEN	SPE	Kappa	MCC	F1 score
Train	LR	0.9519(0.9349–0.9690)	0.8620	0.9281	0.8589	0.3250	0.4248	0.3727
	KNN	0.9998(0.9996–1.0000)	0.9991	1.0000	0.9991	0.9898	0.9899	0.9903
	SVM	0.9514(0.9339–0.9689)	0.8871	0.8954	0.8867	0.3691	0.4528	0.4120
	RF	1.0000(1.0000–1.0000)	1.0000	1.0000	1.0000	1.0000	1.0000	1.0000
	CatBoost	0.9429(0.9219–0.9639)	0.9347	0.8170	0.9402	0.4949	0.5350	0.5252
	XGBoost	1.0000(0.9999,1.0000)	0.9983	1.0000	0.9982	0.9799	0.9801	0.9808
	AdaBoost	0.8141(0.7884,0.8398)	0.6639	0.9216	0.6520	0.1260	0.2437	0.1950
	GBM	0.9895(0.9837–0.9954)	0.9700	0.9281	0.9719	0.7168	0.7354	0.7320
	NNet	0.9507(0.9340–0.9675)	0.8975	0.8889	0.8979	0.3933	0.4704	0.4338
Validation	LR	0.9608(0.9369–0.9847)	0.8721	1.0000	0.8665	0.3516	0.4618	0.3951
	KNN	0.9280(0.8525–1.0000)	0.8407	0.9375	0.8365	0.2801	0.3902	0.3297
	SVM	0.9625(0.9396–0.9855)	0.9295	0.9375	0.9292	0.4960	0.5608	0.5263
	RF	0.9479(0.9099–0.9858)	0.8799	0.9375	0.8774	0.3520	0.4486	0.3947
	CatBoost	0.9562(0.9307–0.9818)	0.8486	1.0000	0.8420	0.3080	0.4267	0.3556
	XGBoost	0.9659(0.9408–0.9911)	0.9138	0.9375	0.9128	0.4414	0.5185	0.4762
	AdaBoost	0.6113(0.4834–0.7392)	0.7676	0.4375	0.7820	0.0703	0.1048	0.1359
	GBM	0.9477(0.8962–0.9993)	0.9608	0.8125	0.9673	0.6145	0.6316	0.6341
	NNet	0.9535(0.9250–0.9821)	0.8303	1.0000	0.8229	0.2796	0.4032	0.3299
Test	XGBoost	0.9855(0.9712–0.9998)	0.9513	1.0000	0.9498	0.5253	0.5968	0.5455

Train training set, Validation validation set, Test testing set, AUC area under the curve, ACC accuracy, SEN sensitivity, SPE specificity, MCC Matthews correlation coefficient

terms of both AUC and MCC. Based on our evaluation metrics, we believe that the XGboost model demonstrated the best performance.

The evaluation metrics of XGBoost model based on testing set are shown in Table 2. The ROC curve and decision curve analysis for the XGBoost model of the testing set are shown in Fig. 3. With AUC value of 0.9855 (95%CI: 0.9712–0.9998) and MCC value of 0.5968, the model constructed using XGBoost algorithm shows good discrimination, generalization in the testing set. The decision curve analysis showes that when the threshold probability is less than 76%, the net clinical benefit of this model in the testing set is greater than 0. It indicated a high potential for clinical application.

Interpretation of the model

To demonstrate the importance of features, we generated a SHAP summary plot for the 13 clinical features affecting the XGBoost model, as shown in Fig. 4. In addition, We plotted SHAP force analysis diagrams for two samples from the validation set using the XGBoost model to demonstrate individualized predictions. Figure 5A presents one case where no fungal infection occurred after surgery. The patient is a 51-year-old male, no DM or history of malignancy, and no being bedridden. Her admission WBC is 3.56×10^{9}/L, with no preoperative ureteral stent placement. The surgery lasted 35 min with no fever occurred after surgery. The postoperative Neu is 8.86×10^{9}/L. The duration of antibiotic therapy is

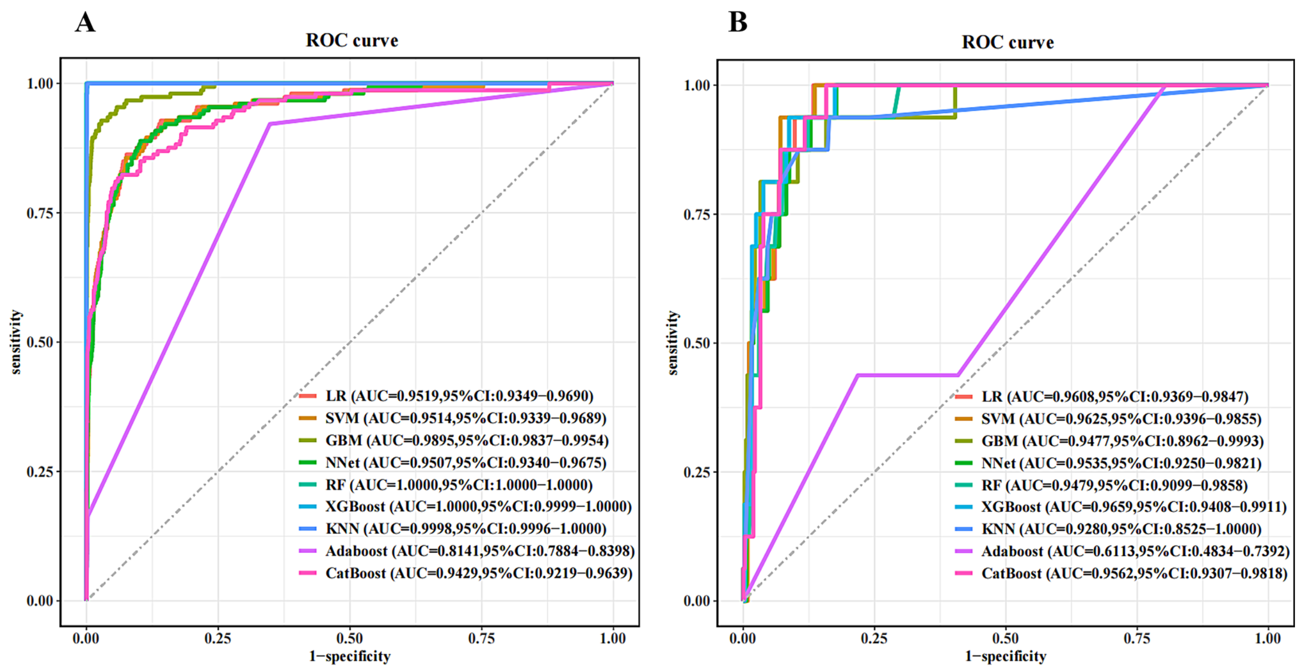

Fig. 2 The ROC curves for each model in the training and validation sets. **A** ROC curves in the training set. **B** ROC curves in the validation set. The AUC value of the XGBoost model is the highest, at 0.9659 (0.9408–0.9911)

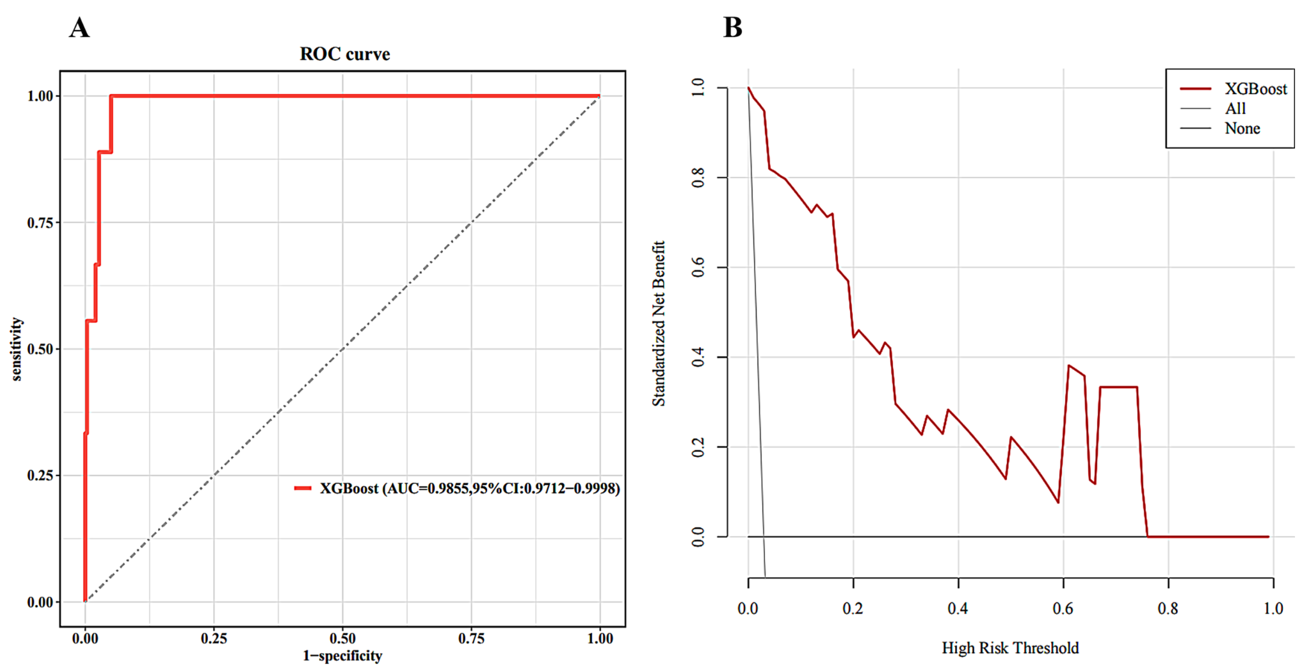

Fig. 3 The ROC curve and decision curve analysis of the XGBoost model in the testing set. **A** ROC curve of the XGBoost model in the testing set. The AUC value is 0.9855 (0.9712–0.9998). **B** Decision curve analysis of the XGBoost model in the testing set. The decision curve analysis showes that when the threshold probability is less than 76%, the net clinical benefit of this model in the testing set is greater than 0

eight days. No carbapenem antibiotics were used during hospitalization, which lasted for eight days. The postoperative stent duration is four weeks. Our model predicted no fungal infection occurred, which aligned with the actual result. Figure 5B presents another case, where fungal infection occurred after surgery. The patient is a 61-year-old female with a history of endometrial cancer. No DM or being bedridden. Her admission WBC is 10.12×10^9/L, with no preoperative ureteral stent placement. The surgery lasted 115 min with postoperative fever occurred. The postoperative Neu is 8.19×10^9/L. The duration of antibiotic therapy is eight days. She

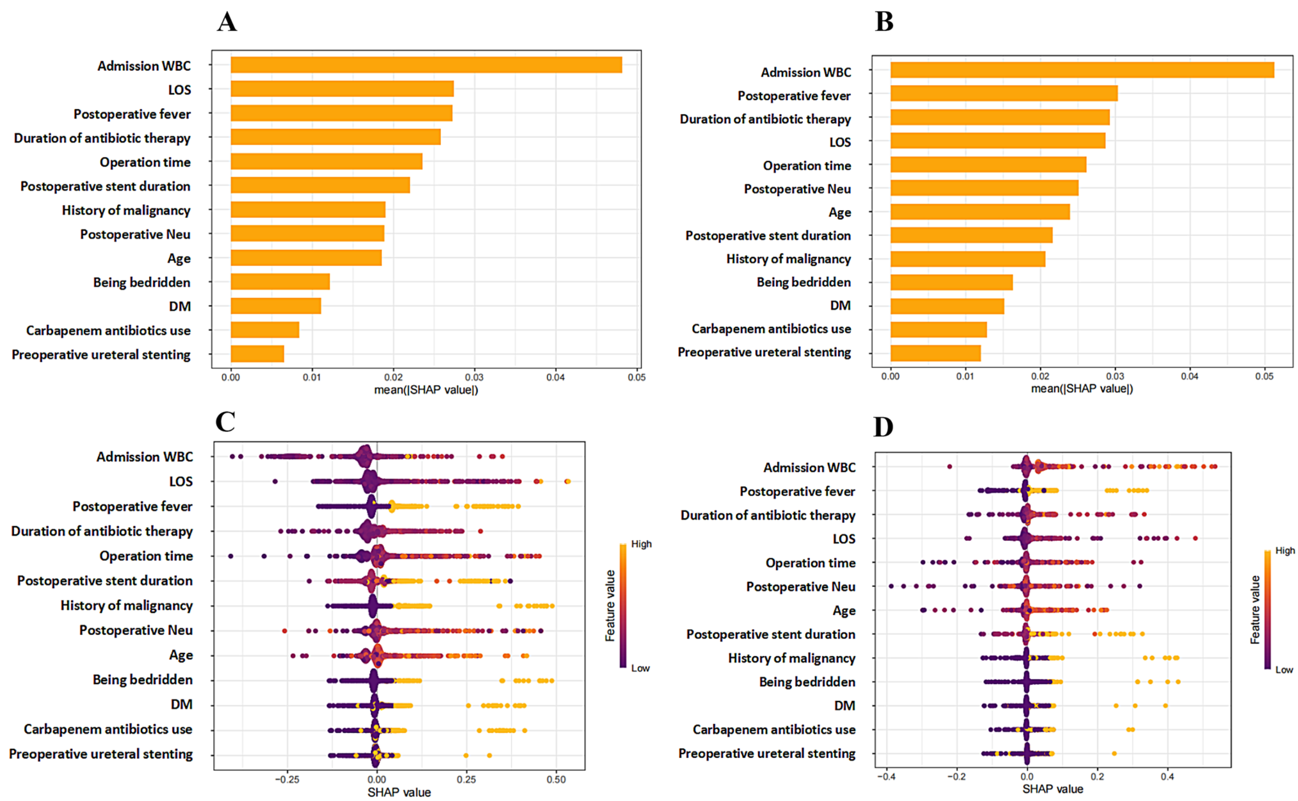

Fig. 4 The SHAP summary plots for the 13 clinical features affecting the XGBoost model. **A** Feature importance ranking according to SHAP in the training set. **B** Feature importance ranking according to SHAP in the validation set. **C** Summary plot of SHAP values in the training set. **D** Summary plot of SHAP values in the validation set. From top to bottom, the influence of features on the model gradually decreases. If the horizontal sample distribution is relatively scattered, it means that the feature has a greater impact. Yellow dots represent higher observation values, while purple dots represent lower observation values

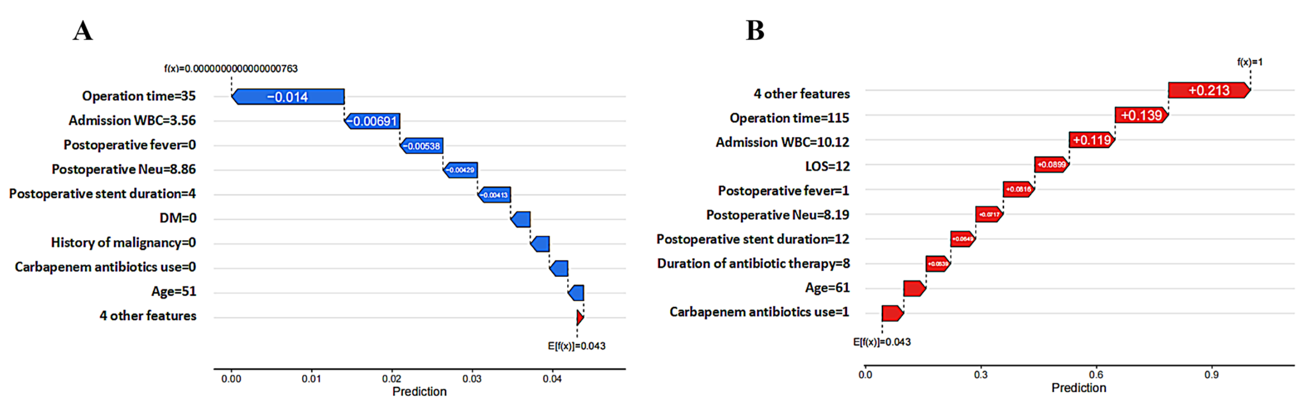

Fig. 5 SHAP force plots for two cases in the validation set. **A** SHAP force plot for a case where no fungal infection occurred postoperatively. **B** SHAP force plot for a case where fungal infection occurred postoperatively. The red bar represents positive impact, while the blue bar represents negative impact. The length of the bar chart is directly proportional to the magnitude of the impact

received carbapenem antibiotics and was hospitalized for 12 days. The postoperative stent duration is 12 weeks. Our model predicted fungal infection occurred, which matched the actual outcome.

Discussion

By applying LASSO regression to screen clinical features, we identified that age, DM, history of malignancy, being bedridden, admission WBC, preoperative ureteral stenting, operation time, postoperative fever, postoperative Neu, carbapenem antibiotics use, duration of antibiotic therapy, LOS, and postoperative stent duration were risk factors for fungal infections in patients following F-URL. Comparing the performance of 9 prediction models, we found that the model constructed using XGBoost algorithm had the best performance.

Traditional perspectives suggest that fungal urinary tract infections (UTIs) constitute less than 5% of all UTIs [25], but in recent years, the proportion of fungal UTIs has shown a growing trend [11]. Studies have demonstrated that urolithiasis, surgical interventions, and catheterization are key risk factors for fungal infections [2]. Early symptoms of fungal infections are nonspecific, and fungal culture, while considered the diagnostic gold standard, suffers from drawbacks such as contamination, low sensitivity, and long processing times, often leading to missed diagnoses and delayed treatment, thus increasing costs [26]. Catheter-associated fungal infections in the urinary tract often involve biofilm formation, which enhances pathogenicity and makes the infection highly resistant to antifungal drugs and host immune factors, leading to prolonged and difficult-to-treat infections [27]. Removing underlying causes is the primary step in treating fungal infections of the urinary tract [28]. Therefore, building a risk prediction model for fungal infection following F-URL and evaluating infection risks are of critical clinical significance in identifying high-risk patients for early diagnosis and timely removal of controllable risk factors.

Currently, six studies have investigated the risk factors for fungal urinary tract infections [5, 6, 10–13,], with two focusing on preoperative urolithiasis patients [12–14] and one on postoperative urology patients [9]. However, previous studies mostly used bacterial UTI patients as the control group [9–12], included fewer variables, reached inconsistent conclusions, and did not establish prediction models. Traditional methods using univariate or multivariate logistic regression to explore risk factors lack the ability to handle datasets with multicollinearity. Compared to traditional methods, the machine learning algorithms used in this study offer significant advantages in diagnostic and prognostic applications [29].

XGBoost is based on the gradient lifting decision tree algorithm, using the second-order Taylor formula expansion, and adding regularization to the objective function to control the complexity of the model. Compared with other algorithms, XGBoost has certain advantages. For example, it can achieve efficient and accurate analysis of large and complex data sets by adjusting parameters [30]. In recent years, xgboost algorithm has been gradually applied to the medical field [31], especially in the prediction of sepsis [32]. Through the use of diagnostic and prognostic algorithms for faster diagnosis and personalized medical treatment, it also provides the possibility for future digital medical treatment [33]. However, the application of xgboost model also has certain limitations. For example, most studies are single center or single database studies, and the results may lack external data authentication to improve persuasion [32]. In addition, learning software such as Python and R language is relatively difficult, and the lack of analyzable data also affects the further promotion of xgboost in the medical field [34].

Our study shows that age is a risk factor for fungal infections in patients after F-URL. Previous studies also believed that the elderly were associated with the risk of urinary fungal infection [9–14]. Elderly patients have diminished physical resilience and weakened immune functions, reducing the defense mechanisms of the urethral mucosa, which makes fungi originally colonizing the perineum more likely to become opportunistic pathogens causing urinary tract infections [2]. Additionally, with advancing age, conditions such as benign prostatic hyperplasia and neurogenic bladder become more prevalent, leading to urine retention or increased need for catheterization, thereby raising the risk of postoperative fungal infections [35].

Previous studies indicate that immune mechanisms play a crucial role in preventing fungal infections [36]. Our study reveals that DM is a risk factor for fungal infections after F-URL. Several studies [9, 10, 12–14] also showed that diabetic patients had an increased risk of urinary fungal infection, though differing from the conclusions of Duoyun J et al. [11]. One study found that chronic hyperglycemia impairs monocyte phagocytic function and compromises complement efficacy [37]. Diabetic patients have weakened immune functions, leading to a higher incidence of urinary fungal infections. Furthermore, studies have shown that Candida albicans proliferation is enhanced in acidic environments and in the presence of nitrogenous compounds, increasing pathogenicity, which raises the risk of fungal infections in diabetic patients with azotemia or ketoacidosis [38]. Regulating blood glucose levels is crucial for preventing fungal infections after F-URL.

Our study indicates that patients with a history of malignancy are more prone to fungal infections after F-URL. In addition to cachexia caused by the malignancy itself, chemotherapy can reduce neutrophil levels and weaken immune function, increasing the risk of fungal infections and leading to poor outcomes [39]. Furthermore, postoperative radiation therapy in patients with cervical or prostate cancer often results in complications such as ureteral strictures, leading to the need for prolonged ureteral stent placement, which increases the risk of fungal infections [40]. Some patients with a history of malignancy may have undergone organ transplants and are on long-term immunosuppressive therapy, further raising the risk of fungal infections [41].

The study of Duoyun J et al. [11] concluded that long-term bed rest was a risk factor for urinary fungal infection, but another study of Junfeng Z et al. [10] on the risk factors of urinary fungal infection did not support this point. We believe that in bedridden patients, primary neurological conditions like stroke often impair urinary reflexes and autonomous voiding, making them prone to urine retention and increasing the need for catheterization, which in turn raises the risk of fungal infections [35]. White blood cells and neutrophils are key components of the inflammatory response, and preoperative infections often escalate the level and duration of antibiotic use, suppressing sensitive bacteria and promoting Candida overgrowth, which can lead to microbial imbalance and increased fungal infection rates [42].

In patients with severe obstruction accompanied by infection, rapid increases in creatinine or blood potassium levels often necessitate immediate ureteral stenting or nephrostomy to relieve the obstruction. These invasive urological procedures and catheterizations are associated with an increased risk of fungal infections [27].

Postoperative fever within 48 h is often caused by infection [43]. Postoperative infections escalate the level and duration of antibiotic use, and broad-spectrum antibiotics suppress a wide range of sensitive bacterial populations, allowing resistant fungal species to proliferate, increasing the risk of fungal infections [42]. Additionally, postoperative infections extend the duration of nephrostomy tubes and urinary catheters, further increasing the risk of fungal infections [27].

Our study shows that LOS is a risk factor for fungal infections after urinary tract stone surgery. Previous research suggests that prolonged postoperative hospital stay is related to infectious complications [44], indicating that LOS may reflect the use of antibiotics, which influences the risk of fungal infections.

The use of broad-spectrum systemic antibiotics is one of the primary risk factors for fungal infections [42]. The carbapenem antibiotics used in this study included imipenem, biapenem, and meropenem, all of which are broad-spectrum antibiotics. In clinical practice, it is essential to strictly manage the use of antibiotics and avoid overuse to reduce the risk of multidrug-resistant bacteria and fungal infections.

Previous research has found that the stent duration is a significant risk factor for ureteral stent infections [45]. Our study suggests that the longer the ureteral stent remains, the higher the risk of fungal infections after F-URL. Previous studies have shown that Candida albicans can switch to hyphal growth after contact with biological or non-biological solid surfaces [46]. On surfaces of specific structures like ureteral stents, directional hyphal growth, known as tropism, may occur [47]. Biofilm formation on catheter surfaces is a critical pathogenic factor for Candida albicans. In addition to enhancing pathogenicity, biofilms provide strong resistance to antifungal agents and host immune factors, leading to persistent catheter-related fungal infections in clinical practice [48]. Although current research has developed various methods for the prevention and treatment of catheter-related fungal biofilms, including antifungal lock therapy, antifungal catheter coatings, natural peptide-based products, and methylene blue photodynamic inactivation [46], most of these advancements have primarily been applied to central venous catheters [49, 50]. Therefore, for high-risk patients, the unnecessary stent duration should be minimized to reduce the risk of ureteral stent-related urinary infections, including fungal infections [44]. For patients with severe ureteral stenosis or post-urinary diversion surgery who must have long-term stents, timely replacement of the stent or the use of new antifungal stents should be considered to reduce the risk of fungal infections [49]. When fungal infections associated with a ureteral stent occur, the primary treatment is to remove the ureteral stent [28].

A study has shown that females have a higher risk of ureteral stent infections [51]. However, the relationship between sex and the risk of urinary fungal infections remains controversial [2, 9–14]. This study indicates that females have a higher risk of developing urinary fungal infections. This finding aligns with that of Behzadi P et al. [2] but contrasts with several studies on urinary fungal infection risk factors [9–14], including Duoyun J et al. [11], which found a higher risk of fungal infections in males. This discrepancy may be attributed to some studies using bacterial urinary infection patients as the control group [9–12] and to geographical and selection biases in single-center studies.

Since nearly 50% of the patients in this study had multiple stones, and some patients had stones in multiple locations, we did not analyze the impact of stone location on postoperative fungal infections to ensure statistical scientific rigor. Previous studies on risk factors for fungal infections in patients with urinary stones did not find a significant association between stone location, stone size, and the risk of fungal infection [12, 14]. A study by Jialong L et al. found that patients with staghorn calculi are prone to combined fungal infections [14]. However, since our center uses PCNL or PCNL combined with F-URL to treat staghorn calculi, this study did not include such patients. Future research is needed to explore the risk of fungal infections after F-URL in patients with staghorn calculi and its underlying mechanisms.

The pressure in the collecting system and temperature during furl are the focus of many clinicians [52–54]. In order to maintain the visual field and reduce the temperature, normal saline perfusion is often continued during lithotripsy. However, this may lead to the increase of ithe collecting system pressure, and then lead to bacteria and endotoxin entering the blood circulation through the renal pelvis vein, renal pelvis lymph reflux and other causes of infection [52, 53]. Although the T-UAS can accelerate the drainage of perfusion fluid to a certain extent, thereby reducing the pressure of the collecting system, this reduction is relatively limited [55]. Compared with the T-UAS, the NP-UAS can not only improve stone-free rate, but also effectively prevent high renal pelvic pressure and reduce postoperative infection complications [53, 54]. Our study found that there was a significant difference in the types of sheaths used between the fungal infection group and the non-fungal infection group, but it could not be used as a key factor to predict the risk of fungal infection. It is hoped that future studies can further reveal the internal relationship between the NP-UAS and fungal infection, so as to provide more comprehensive strategies for reducing the risk of postoperative fungal infection.

The study of Kumar GM et al. [56] has confirmed that residual calculi is associated with the risk of postoperative bacterial infection, and more studies are needed to confirm the effect on the risk of postoperative fungal infection.

This study has several advantages. To our knowledge, it is the first to develop a predictive model for the risk of fungal infections following F-URL. In this study, we used LASSO regression to select variables, which reduced overfitting and further improved model performance. The constructed optimal model performed excellently in performance evaluations and holds potential for wider application.

This study has some limitations. As a single-center retrospective study with a limited sample size, it is subject to geographical and selection biases. In order to reduce the risk of over fitting, we did not use smote and other methods to improve the recall rate of a few categories, which may affect the performance of the model to a certain extent. Additionally, it did not analyze the impact of preoperative catheterization, intrarenal pressure, intrarenal temperature, the energy levels applied, different ureteral stent models, or specific types of antibiotics on the risk of fungal infection following flexible ureteroscopy lithotripsy. Preoperative catheterization may increase the risk of postoperative fungal infection in stone patients as an invasive procedure. These missing data during surgery may affect the risk of fungal infection by affecting efficacy and infectious complications. The absence of this part of the data not only increases the heterogeneity, but may also prevent us from exploring the intrinsic relationship of these data to fungal infection and thus provide more comprehensive strategies for reducing the risk of fungal infection. We look forward to exploring the possible influence of these differences on postoperative fungal infection in future studies. Meanwhile, we hope that future prospective studies can employ more standardized treatment protocols to reduce heterogeneity and make the conclusions more reliable. We only used the data of the center as the test set to verify the generalization ability of the model, the constructed model requires further validation with larger sample sizes. Therefore, future studies should involve more comprehensive, multicenter, large-sample prospective research to explore this further.

In summary, this study utilized 13 clinical characteristics to develop a predictive model for the risk of fungal infection following flexible ureteroscopy lithotripsy using nine machine learning methods, followed by validation and evaluation. The XGBoost model developed in this study demonstrated strong predictive ability and clinical applicability. Through shap plots, we demonstrated at an individual level how the XGBoost model can help clinicians early identify patients at high risk of fungal infection after flexible ureteroscopy. The study not only identified key risk factors for postoperative fungal infections after flexible ureteroscopic lithotripsy but also filled a gap in the field of predictive models for the risk of urinary fungal infections. We discussed the underlying mechanisms of these risk factors and proposed preventive measures for controllable risk factors to reduce the incidence of postoperative fungal infections. Moreover, implementing early targeted screening for high-risk populations holds promise for facilitating early diagnosis and timely intervention. These early intervention strategies are expected to significantly decrease the occurrence of postoperative fungal infections, improve patient outcomes, and reduce healthcare costs. The study provides new insights and methodologies for further exploration of risk management in urinary fungal infections.

Abbreviations

URL	Flexible ureteroscopy lithotripsy
LR	Logistic Regression
KNN	k-Nearest Neighbours
SVM	Support Vector Machines
RF	Random Forest
CatBoost	Classification and Regression Trees
XGBoost	eXtreme Gradient Boosting
AdaBoost	Adaptive Boosting
GBM	Gradient Boosting Machines
NNet	Neural Network
BMI	Body mass index
DM	Diabetes mellitus
Immunosuppression	Long-term immunosuppressive therapy
HB	Hemoglobin
WBC	White blood cells
Neu	Neutrophils
ALT	Alanine transaminase
AST	Aspartate transaminase
Scr	Serum creatinine
CSD	Cumulative stone diameter
PSD	Peak stone density
PNS	Percutaneous nephrostomy
UAS	Ureteral access sheath
T-UAS	Traditional ureteral access sheath
NP-UAS	Negative-pressure ureteral access sheath
Ca	Serum calcium
LOS	Length of hospital stay

WHO	World Health Organization
Train	Training set
Validation	Validation set
Test	Testing set
DCA	Decision curve analysis
AUC	Area under the curve
ACC	Accuracy
SEN	Sensitivity
SPE	Specificity
MCC	Matthews correlation coefficient
CSRF	Clinically Significant Residual Fragments

Acknowledgements
Not applicable.

Author contributions
All authors reviewed the manuscript.

Funding
The study does not involve funding support.

Data availability
No datasets were generated or analysed during the current study.

Declarations

Ethics approval and consent to participate
The study was approved by the Ethics Committee of the Second Affiliated Hospital of Zhengzhou University (Approval No.: KY2024194). All study participants have signed informed consent forms. Our research process complies with the requirements of the Helsinki Declaration of the World Medical Association.

Consent for publication
Not applicable.

Competing interests
The authors declare no competing interests.

Author details
[1]Department of Urology, The Second Affiliated Hospital of Zhengzhou University, Zhengzhou 450000, China
[2]The Second Clinical Medical School of Zhengzhou University, No. 2 Jingba Road, Jinshui District, Zhengzhou 450000, China

Received: 9 October 2024 / Accepted: 26 March 2025
Published online: 10 April 2025

References

1. Guohua Z, Zanlin M, Shujie X, et al. A cross-sectional survey of urolithiasis prevalence in China. Chin J Urol. 2015;36(7):528–32. https://doi.org/10.3760/cma.j.issn.1000-6702.2015.07.014.
2. Behzadi P, Behzadi E, Ranjbar R. Urinary tract infections and Candida albicans. Cent European J Urol. 2015;68(1):96–101. https://doi.org/10.5173/ceju.2015.01.474.
3. Li Y, Xia Z, Li Z, et al. Distribution and drug resistance analysis on fungal infection in the urinary tract. Modern Prev Med. 2013;40:1330–1331+1335.
4. Yang J, Feng W, XI Z, et al. Analysis of epidemiology and relevant risk factors of patients with Nosocomial Fungal Infection in Uninary System. Chin J Health Lab Technol. 2011;21:2219–21.
5. Beam AL, Kohane IS. Big data and machine learning in health care. Jama. 2018;319(13):1317–18. https://doi.org/10.1001/jama.2017.18391.
6. Osta E, Ramirez R, Alan J, et al. Use of artificial intelligence in diagnosis and treatment of recurrent nephrolithiasis. J Urol. 2024;211:e1038.
7. Deol ES, Lu D, Oguz I, et al. Real-time kidney stone segmentation during distinct ureteroscopic tasks using a computer vision model. J Urol. 2024;211:e110.
8. Maciolek K, Lu D, Oguz I, et al. Automated analysis of stone dust during ureteroscopy to predict stone free status using computer vision models. J Urol. 2024;211:e552.
9. Haiqing D, Xiaobin Z, Fan C, et al. Distribution and risk factors analysis of pathogenic fungus causing fungal infectionin urology department. Med J Wuhan Uni. 2017;38(03):467–70. https://doi.org/10.14188/j.1671-8852.2017.03.026.
10. Junfeng Z, Ziyang Z, Wangchao H, et al. Analysis of clinical characteristics and risk factors of nosocomial fungal urinary tract infection in ICU. Chin J Mycol. 2022;17(4):273–77. https://doi.org/10.3969/j.issn.1673-3827.2022.04.003.
11. Duoyun J. The investigation of the fungal urinary tract infection and risk factor analysis. Guangxi Medical University, 2016. https://doi.org/10.7666/d.D01000147.
12. Junbing Y, Lihong Y, Jiansong H, et al. Analysis of microflora distribution, drugsusceptibility, and risk factors of fungal infection in patients with urolithiasi. Chin J Mycol. 2021;16(6):384–387,402. https://doi.org/10.3969/j.issn.1673-3827.2021.06.006.
13. Qiu Y, Hong L. Characteristics and risk factors of fungal infection after urinary surgery. Chin J Mycol. 2023;18(1):8–11,18. https://doi.org/10.3969/j.issn.1673-3827.2023.01.002.
14. Jialong L, Jiamei G, Xiaoling Z. Pathogen characteristics, susceptible factors and preventive measures of urethral fungal infection in patients with urolithiasis. J Hubei Uni Sci Technol (Med Sci). 2024;38(02):152–55. https://doi.org/10.16751/j.cnki.2095-4646.2024.02.0152.
15. Alberti KG, Zimmet PZ. Definition, diagnosis and classification of diabetes mellitus and its complications. Part 1: diagnosis and classification of diabetes mellitus provisional report of a WHO consultation. Diabet Med. 1998;15(7):539–53. https://doi.org/10.1002/(SICI)1096-9136(199807)15:7.
16. Use of Glycated Haemoglobin (HbA1c) in the Diagnosis of Diabetes Mellitus: abbreviated Report of a WHO Consultation. Geneva: World Health Organization; 2011.
17. Zanetta VC, Rosman BM, Bromley B, et al. Variations in management of mild prenatal hydronephrosis among maternal-fetal medicine obstetricians, and pediatric urologists and radiologists. J Urol. 2012;188(5):1935–39. https://doi.org/10.1016/j.juro.2012.07.011.
18. Stephenson C, Mohabbat A, Raslau D, et al. Management of common postoperative complications. Mayo Clin Proc. 2020;95(11):2540–54. https://doi.org/10.1016/j.mayocp.2020.03.008.
19. Bichler KH, Eipper E, Naber K. Infektinduzierte Harnsteine [Infection-induced urinary stones]. Urologe A. 2003;42(1):47–55. https://doi.org/10.1007/s00120-002-0272-5
20. Assimos D, Krambeck A, Miller NL, et al. Surgical management of stones: american urological association/endourological society guideline, PART I. J Urol. 2016;196(4):1153–60. https://doi.org/10.1016/j.juro.2016.05.090.
21. Krcmery S, Dubrava M, Krcmery Jr V. Fungal urinary tract infections in patients at risk. Int J Antimicrob Agents. 1999;11(3-4):289–91. https://doi.org/10.1016/s0924-8579(99)00032-1.
22. Cai W, van der Laan M, Nonparametric bootstrap inference for the targeted highly adaptive least absolute shrinkage and selection operator (LASSO) estimator. Int J Biostat. August 10, 2020. https://doi.org/10.1515/ijb-2017-0070.
23. Chicco D, Jurman G. The advantages of the matthews correlation coefficient (MCC) over F1 score and accuracy in binary classification evaluation. BMC Genomics. 2020;21(1):6. https://doi.org/10.1186/s12864-019-6413-7.
24. Lundberg SM, Erion G, Chen H, et al. From local explanations to global understanding with explainable ai for trees. Nat Mach Intell. 2020;2:56–67.
25. Sobel JD, Vazquez JA. Fungal infections of the urinary tract. World J Urol. 1999;17(6):410–14. https://doi.org/10.1007/s003450050167.
26. Mendonça A, Santos H, Franco-Duarte R, et al. Fungal infections diagnosis—past, present and future. Res Microbiol. 2022;173(3):103915. https://doi.org/10.1016/j.resmic.2021.103915.
27. Fanning S, Mitchell AP. Fungal biofilms. PLoS Pathog. 2012;8(e1002585). https://doi.org/10.1371/journal.ppat.1002585.
28. Dariane C, Cornu JN, Esteve E, et al. Infections fongiques et matériel urétéral: quelle prise en charge? [Fungal infections and ureteral material: how to manage?]. Prog Urol. 2015;25(6):306–11. https://doi.org/10.1016/j.purol.2015.01.015.
29. He J, Baxter SL, Xu J, et al. The practical implementation of artificial intelligence technologies in medicine. Nat Med. 2019;25(1):30–36. https://doi.org/10.1038/s41591-018-0307-0.

30. Lundberg SM, Erion G, Chen H, et al. From local explanations to global understanding with explainable ai for trees. Nat Mach Intell. 2020;2(1):56–67. https://doi.org/10.1038/s42256-019-0138-9.
31. Dodig S, Čepelak I, Dodig M. Are we ready to integrate advanced artificial intelligence models in clinical laboratory? Biochem Med (Zagreb). 2025;35(1):010501. https://doi.org/10.11613/BM.2025.010501.
32. Tądel K, Dudek A, Bil-Lula I. AI algorithms for modeling the risk, progression, and treatment of sepsis, including early-onset sepsis-a systematic review. J Clin Med. 2024 [Published 2024 Oct 7];13(19):5959. https://doi.org/10.3390/jcm13195959.
33. Ahmed Z, Mohamed K, Zeeshan S, Dong X. Artificial intelligence with multi-functional machine learning platform development for better healthcare and precision medicine. Database (Oxford). 2020; 2020:baaa010. https://doi.org/10.1093/database/baaa010.
34. van Panhuis WG, Paul P, Emerson C, et al. A systematic review of barriers to data sharing in public health. BMC Public Health. 2014;14:1144. https://doi.org/10.1186/1471-2458-14-1144.
35. Verduyn Lunel FM, Meis JF, Voss A. Nosocomial fungal infections: candidemia. Diagn Microbiol Infect Dis. 1999;34(3):213–20. https://doi.org/10.1016/s0732-8893(99)00035-8.
36. Desai JV, Lionakis MS. The role of neutrophils in host defense against invasive fungal infections. Curr Clin Microbiol Rep. 2018;5(3):181–89. https://doi.org/10.1007/s40588-018-0098-6.
37. Pearson-Stuttard J, Blundell S, Harris T, et al. Critchley J. Diabetes and infection: assessing the association with glycaemic control in population-based studies. Lancet Diabetes Endocrinol. 2016;4(2):148–58. https://doi.org/10.1016/S2213-8587(15)00379-4.
38. Abaitua F, Rementería A, Millan RS, et al. In vitro survival and germination of Candida albicans in the presence of nitrogen compounds. Microbiology (Reading). 1999;145(Pt 7):1641–1647. https://doi.org/10.1099/13500872-145-7-1641.
39. Puig-Asensio M, Ruiz-Camps I, Fernández-Ruiz M, et al. Epidemiology and outcome of candidaemia in patients with oncological and haematological malignancies: results from a population-based surveillance in Spain. Clin Microbiol Infect. 2015;21(5). https://doi.org/10.1016/j.cmi.2014.12.027.
40. Lee KB, Lee JM, Ki KD, et al. Comparison of adjuvant chemotherapy and radiation in patients with intermediate risk factors after radical surgery in FIGO stage IB-IIA cervical cancer. Int J Gynecol Cancer. 2008;18(5):1027–31. https://doi.org/10.1111/j.1525-1438.2007.01136.x.
41. Keighley CL, Pope A, Marriott DJE, et al. Risk factors for candidaemia: a prospective multi-centre case-control study. Mycoses. 2021;64(3):257–63. https://doi.org/10.1111/myc.13211.
42. Groot AJ, Geubbels EL, Beaumont MT, et al. Ziekenhuisinfecties en risicofactoren op de intensive-careafdelingen van 16 Nederlandse ziekenhuizen; resultaten van surveillance als indicator voor zorgkwaliteit [Hospital infections and risk factors in the intensive care units of 16 Dutch hospitals, results of surveillance of quality assurance indicators]. Ned Tijdschr Geneeskd. 2001;145:1249–54.
43. Pratt RJ, Pellowe C, Loveday HP, et al. The epic project: developing national evidence-based guidelines for preventing healthcare associated infections. Phase I: guidelines for preventing hospital-acquired infections. Department of Health (England) J Hosp Infect. 2001:47:S3–S82. https://doi.org/10.1053/jhin.2000.0886.
44. Zhang X, Wei X, Lin S, et al. Predictive model for prolonged hospital stay risk after gastric cancer surgery. Front Oncol. 2024;14:1382878. 2024 Aug 6. https://doi.org/10.3389/fonc.2024.1382878.
45. Kehinde EO, Rotimi VO, Al-Awadi KA, et al. Factors predisposing to urinary tract infection after J ureteral stent insertion. J Urol. 2002;167:1334–37.
46. Kumamoto CA. Molecular mechanisms of mechanosensing and their roles in fungal contact sensing. Nat Rev Microbiol. 2008;6(9):667–73. https://doi.org/10.1038/nrmicro1960.
47. Brand A, Shanks S, Duncan VM, et al. Hyphal orientation of Candida albicans is regulated by a calcium-dependent mechanism. Curr Biol. 2007;17:347–52.
48. Fanning S, Mitchell AP. Fungal biofilms. PLoS Pathog. 2012;8:e1002585. https://doi.org/10.1371/journal.ppat.1002585.
49. Liu N, Wang C, Su H, et al. Strategies in the discovery of novel antifungal scaffolds. Future Med Chem. 2016;8(12):1435–54. https://doi.org/10.4155/fmc-2016-0020.
50. Kovács R, Majoros L. Antifungal lock therapy: an eternal promise or an effective alternative therapeutic approach? Lett Appl Microbiol. 2022;74(6):851–62. https://doi.org/10.1111/lam.13653.
51. Farsi HM, Mosli HA, Al-Zemaity MF, et al. Bacteriuria and colonization of double-pigtail ureteral stents: long-term experience with 237 patients. J Endourol. 1995;9(6):469–72. https://doi.org/10.1089/end.1995.9.469.
52. Dybowski B, Bres-Niewada E, Rzeszutko M, et al. Risk factors for infectious complications after retrograde intrarenal surgery - a systematic review and narrative synthesis. Cent European J Urol. 2021;74(3):437–45. https://doi.org/10.5173/ceju.2021.250.
53. Zhu Z, Cui Y, Zeng F, Li Y, Chen Z, Hequn C. Comparison of suctioning and traditional ureteral access sheath during flexible ureteroscopy in the treatment of renal stones. World J Urol. 2019;37(5):921–29. https://doi.org/10.1007/s00345-018-2455-8.
54. Qian X, Liu C, Hong S, et al. Application of suctioning ureteral access sheath during flexible ureteroscopy for renal stones decreases the risk of postoperative systemic inflammatory response syndrome. Int J Clin Pract. 2022;2022:9354714. 2022 Mar 12. https://doi.org/10.1155/2022/9354714.
55. Noureldin YA, Kallidonis P, Ntasiotis P, Adamou C, Zazas E, Liatsikos EN. The effect of irrigation power and ureteral access sheath diameter on the maximal intra-pelvic pressure during ureteroscopy: in vivo experimental study in a live anesthetized pig. J Endourol. 2019;33(9):725–29. https://doi.org/10.1089/end.2019.0317.
56. Kumar GM, Nirmal KP, Kumar GS. Postoperative infective complications following percutaneous nephrolithotomy. Urol Ann. 2021;13(4):340–45. https://doi.org/10.4103/UA.UA_153_20.

Publisher's Note